



ADA172728

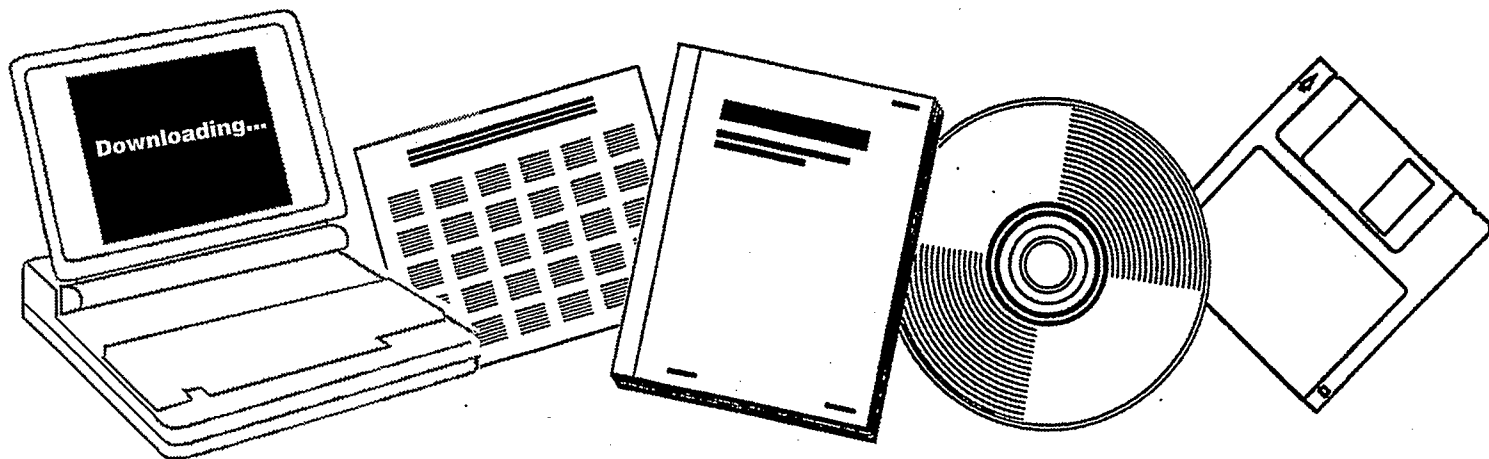
NTIS

One Source. One Search. One Solution.

CHEMISORPTION OF CO, NO AND H₂ ON TRANSITION METAL-TITANIA THIN FILM MODEL CATALYSTS

TEXAS UNIV. AT AUSTIN. DEPT. OF
CHEMISTRY

01 SEP 1986



U.S. Department of Commerce
National Technical Information Service

<div style="border: 1px solid black; border-radius: 50%; padding: 20px; display: inline-block;"> AD-A172 728 </div>	DTIC ACCESSION NUMBER		PHOTOGRAPH THIS SHEET CHEMISORPTION OF CO, NO and H ₂ ON TRANSITION METAL- TITANIA THIN FILM MODEL CATALYSTS (a)	<div style="border: 1px solid black; border-radius: 50%; width: 40px; height: 40px; display: flex; align-items: center; justify-content: center;"> 1 </div>
		LEVEL	1 Sept. 86	INVENTORY
		DOCUMENT IDENTIFICATION		

DISTRIBUTION STATEMENT A
Approved for public release;
Distribution Unlimited

DISTRIBUTION STATEMENT

ACCESSION FOR	
NTIS GRA&I	<input checked="" type="checkbox"/>
DTIC TAB	<input type="checkbox"/>
UNANNOUNCED	<input type="checkbox"/>
JUSTIFICATION	
BY	
DISTRIBUTION /	
AVAILABILITY CODES	
DIST	AVAIL AND/OR SPECIAL
A-1	

QUALITY
INSPECTED
1

DTIC
ELECTE
OCT 16 1986
S **D**

DATE ACCESSIONED

DATE RETURNED

REGISTERED OR CERTIFIED NO.

86 10 14 055

DATE RECEIVED IN DTIC

PHOTOGRAPH THIS SHEET AND RETURN TO DTIC-DDAC

AD-A172 728

Chemisorption of CO, NO and H₂
on Transition Metal-Titania Thin Film Model Catalysts^(a)

1 Sept. 1986

D. N. Belton^(b), Y.-M. Sun^(c) and J. M. White

Department of Chemistry

University of Texas

Austin, TX 78712

Contract N00014-83-K-0582

(a) Supported in part by the Office of Naval Research

(b) Present address: Physical Chemistry Department, GM Research
Laboratories, Warren, MI 48090

(c) Present address: Department of Chemistry and Chemical Engineering,
Tsinghua University, Beijing, People's Republic of
China

ABSTRACT

Chemisorption on thin film models of Rh/TiO₂ and Pt/TiO₂ catalysts before and after encapsulation with TiO_x ($1.0 \leq x \leq 1.2$) is reported. TiO_x blocks adsorption sites and induces new desorption states. A CO desorption peak, assigned to CO on Rh atoms perturbed by TiO_x, is observed at 325 K after adsorption at 120K on a TiO_x-covered Rh/TiO₂ surface. CO adsorbed at 285 K onto the encapsulated Rh/TiO₂ surfaces shows a new 685 K CO desorption state attributed to an activated form of CO with a weakened C-O bond. NO desorbs from clean Rh overlayers with a profile most like Rh(110). On encapsulated Rh surfaces N₂O is the major desorption product. Compared to bulk Pt, desorption experiments show suppressed H₂ adsorption capacity for thin (<2 ML) Pt layers in contact with, but not encapsulated by, TiO_x. For thin layers of Pt on fully oxidized TiO₂ layers there is no reduction of H₂ chemisorption. The results suggest bonding between Ti and Pt which affects H₂ chemisorption even though no Pt surface sites are blocked.

I. INTRODUCTION

Over the last seven years strong metal support interactions (SMSI) have been extensively investigated in powder and model catalyst systems [1-13]. These investigations are predated by a number of important earlier reports [14-18]. An excellent review of the work prior to 1981 was compiled by Bond and Burch [19]. Model catalyst studies (mostly transition metals on titania) conducted after 1981 have convincingly demonstrated that SMSI involves, perhaps not exclusively, encapsulation of the active metal [9,10,20-22]. Although controversy exists about the detailed mechanism of migration, most investigators now agree that for working transition metal catalysts supported on titania in the SMSI state, the transition metal is partially covered by suboxides of Ti. Our previous work demonstrated that encapsulation suppresses hydrogen and carbon monoxide chemisorption, and that restoration occurred when the encapsulating layer was removed [22]. Those results were obtained on model catalysts formed from vapor deposited Rh on oxidized Ti. The work reported here extends those results by examining in more detail the chemisorption of CO, NO and H₂ on reduced and oxidized forms of titania. These systems were selected because they model SMSI catalysts and the results can be connected to widely studied systems.

Our purpose was to look carefully for interactions of TiO_x with chemisorbed molecules to gain insight into the catalytic properties of SMSI catalysts. Dwyer et al. showed that TiO_x on Pt inhibits CO chemisorption by a site blocking mechanism [23]. However, simple site blocking by an inert adsorbate is not sufficient to fully explain SMSI. For example, the fact that catalysts in the SMSI state exhibit increased reactivity and higher molecular weight product distributions for CO hydrogenation indicates that more than simple site blocking of CO and H₂ adsorption is involved [19,24].

The results reported here show that encapsulation has a profound effect on the desorption characteristics of both CO and NO. In addition to blocking sites, TiO_x changes the bonding of both CO and NO adsorbed on Rh. On Pt, encapsulated with TiO_x , H_2 desorption from nearest-neighbor Pt atoms is affected.

II. EXPERIMENTAL

The experiments were performed in a turbo-pumped system equipped with Auger electron spectroscopy (AES), static secondary ion mass spectrometry (SSIMS) and temperature programmed desorption (TPD) capabilities. The model catalysts were composed of Rh (or Pt) layers vapor deposited onto an oxidized Ti(0001) single crystal (typically at 120 K). The oxide overlayer was prepared by exposing the Ti to 5×10^{-7} Torr of O_2 at 775 K for approximately 30 minutes. The AES lineshape of the Ti(418) peak and O/Ti ratios were used to characterize the TiO_2 layer. Attenuations of the Ti and O AES signals were used to estimate metal overlayer thicknesses. For the deposited Rh and Pt we estimate that about 20% of the overlayer was present as three dimensional islands on an otherwise uniform layer. Encapsulated metal layers were prepared by annealing to temperatures above 650 K. The encapsulation process was characterized with AES and SSIMS. The concentration of surface TiO_x depends on both annealing time and temperature [10,22]. Encapsulation was not observed below 600 K.

III. RESULTS

III.1 CO on Rh/ TiO_2

Metal-support interactions have been discussed in terms of the CO chemisorption properties of the supported metal; in the SMSI state CO

chemisorption is suppressed but CO hydrogenation activity is high.[1] Intuitively one might suppose that new CO adsorption sites, created by the presence of TiO_x , are responsible for the enhancement in CO hydrogenation rates observed in metal-titania systems.[24,25] The interaction of CO with TiO_x is properly characterized by comparison with CO adsorption characteristics in the absence of encapsulation. Earlier work [26] suggested that a structural rearrangement of the Rh overlayer occurred prior to encapsulation. Characterization of this rearrangement was necessary to assure that its effects were properly disentangled from encapsulation-mediated events.

Since TiO_x segregation rates vary inversely with the Rh layer thickness, a thick (120 Å) Rh layer was used to minimize encapsulation during several CO desorption experiments (maximum TPD temperatures of 620 K). After deposition of the 120 Å Rh layer onto the oxidized Ti substrate, CO (10 L, at 120 K) was adsorbed before any annealing. In the TPD spectrum (Fig. 1a) there was a broad CO desorption peak at 485 K. The desorption temperature and width are within the range observed on Rh single crystals [27-30]; however, the single crystal Rh desorption peak shapes are typically more skewed toward lower temperatures. During the first desorption experiment, the sample temperature reached 620 K, i.e. the Rh was annealed briefly. After another 10 L CO exposure, the desorption spectrum (Fig. 1b) decreased in area, changed in shape, and shifted to slightly higher temperature (at the peak). The shape of Fig. 1b more nearly resembles CO desorption from Rh single crystal surfaces than Fig. 1a. The low temperature tail and sharp drop at high temperature are characteristic of CO desorption from most Rh single crystals. Although CO desorption from Rh is not strongly structure sensitive, the low temperature shoulder on Rh(111) is

6

more pronounced than observed here, suggesting that the annealed Rh overlayer is more like Rh(100) or Rh(110).

AES data (Figs. 1c and 1d) confirm that the results of Figs. 1a and 1b were not affected by encapsulation. Immediately after deposition of the Rh overlayer, the only species observable, other than Rh, were oxygen and possibly carbon, present due to CO adsorption from the background gases during the Rh deposition. Since saturation CO exposures were studied, background CO adsorption did not affect the final result. After completion of the desorption experiments, AES data (Fig. 1d) showed neither oxygen nor titanium, indicating that during the desorption experiments no encapsulation occurred and there was no massive islanding of the Rh overlayer to expose the substrate. No other foreign atoms were detected by AES. Thus, the decreased adsorption observed in Fig. 1b (compared to 1a) is interpreted as a loss in Rh surface area. According to this interpretation, the as-deposited overlayer was comprised of three dimensional Rh islands present on top of a continuous Rh film. This roughness leads to Rh surface areas that are larger than the geometric area of the substrate. Annealing to 620 K removed some of the roughness, thereby decreasing the surface area and giving CO desorption spectra more nearly resembling those from Rh single crystals.

To eliminate these particular morphology changes from encapsulation effects, samples were annealed to 550 K prior to CO desorption experiments. This temperature was chosen because it was below the temperature where Rh/TiO₂ began to encapsulate and was high enough to give (reproducibly) a CO spectrum like that of Fig. 1b. In the remainder of this paper a "clean Rh/TiO₂ sample" refers to a sample annealed at 550 K.

To study the effect of TiO_x on CO adsorption, saturation CO exposures

were desorbed from Rh/TiO₂ samples with various TiO_x coverages. The latter could be increased by annealing to successively higher temperatures ($600 \leq T \leq 760$ K) prior to CO adsorption at 120 K (Fig. 2). AES established the TiO_x coverage [10]. The upper limit of the temperature ramps in TPD was 620 K in order to minimize encapsulation during TPD. Control experiments established that no CO desorption occurred above 620 K.

According to Fig. 2, TiO_x affects CO desorption profiles in two ways. First, the total CO desorption peak area is reduced as the TiO_x coverage is increased. Second, a new low temperature CO desorption peak (labeled β) grows in as a function of TiO_x coverage. The β desorption state is most notable after annealing to 760 K (Fig. 2d). The dashed line is a rough decomposition to reflect the clean Rh component and the broad lower temperature component. The clean surface peak was extracted by scaling down spectrum 2a with the assumption that the β component does not contribute significantly to desorption at 480 K. The β region may be composed of more than one peak, but further decomposition is not possible. The β desorption maximizes some 150 K below CO desorption from Rh single crystal surfaces [27,28], indicating desorption from highly perturbed Rh atoms (possibly including Ti-O-Rh species). CO desorption from clean TiO₂ (no Rh) peaked at ~ 180 K, establishing that β is not desorption from the titania.

The correlation of CO desorption peak areas with Ti(418)/Rh(304) AES peak-to-peak height ratios is given in Fig. 2B. For submonolayer amounts of TiO_x, the Ti/Rh AES ratios are taken to be linear in TiO_x coverage. Since no calibration was possible, the absolute coverages cannot be determined. Both the α and the total CO peak areas decrease linearly with TiO_x coverage, but there is no detectable shift of the peak temperature of the α state. This is strong evidence that simple site blocking is one important mechanism

5

by which TiO_x inhibits CO adsorption. The β -CO peak area (triangles in Fig. 2B) increases with TiO_x coverage.

These results confirm the conclusions of Dwyer et al. [23] regarding the importance of site blocking by TiO_x . The β desorption state has not been, to our knowledge, previously observed in SMSI systems. However, destabilization of CO by coadsorbates has been observed on Rh surfaces. For example, T. W. Root et al. [31] reported that coadsorbed N atoms decreased CO desorption temperatures by 100 K on Rh(111) and work from our laboratory shows a similar effect on Rh(100). [32] In the present case, it is not possible to determine whether the β -CO involves bonding to perturbed Rh atoms or to a more complex surface specie involving Rh, Ti and O. However, TiO_x is clearly responsible for the presence of these adsorption sites that are much less stable than either bridged or linearly bound CO on clean Rh.

TPD after a 10 L CO exposure at a higher temperature (285 K) onto "clean" and annealed (785 K) Rh/ TiO_2 samples are significantly different (Fig. 3). Figure 3a has the shape and peak temperature characteristic of desorption from clean Rh surfaces. To reiterate, the skewing to low temperature and the relatively sharp decay at temperatures above the peak are characteristic of CO desorption from Rh single crystal surfaces. No CO desorbs above 600 K.

Desorption from the sample annealed to 785 K (encapsulated) differed from the clean surface desorption in three distinct ways. First, the total CO desorption peak areas was 50% lower. This result is similar to the site blocking observed at 120 K. The second difference occurs on the low temperature side of the desorption peak where, on the encapsulated surface, the peak at 485 K is much more symmetric than on clean Rh. More quantitatively, the desorption peak half width is 57 K wider for the clean

Rh substrate. For Rh single crystals the low temperature side of the desorption peak has been associated with bridge-bonded CO [33]. If so, bridged sites are blocked on our encapsulated surfaces. While reasonable, this working hypothesis should be tested by studying CO(a) on TiO_x -covered Rh single crystal surfaces using HREELS.

The third important difference in Fig. 3 is the high temperature desorption peak, labeled γ , which appears at 685 K on the encapsulated surface. No desorption is observed above 600 K after dosing at 120 K on an encapsulated surface. This desorption state is not observed from single crystal or polycrystalline Rh surfaces [22,23,27-30]. Since the γ state was not observed when CO was adsorbed at 120 K, its formation is activated. This fact, coupled with its high temperature and broad desorption region, suggests a dissociated adsorption state. The formation of high temperature desorption states has been observed for a number of systems including potassium-covered Ni [34]. These states are commonly attributed to dissociated CO, or at least an adsorbed species with reduced C-O bond order.

Comparing Figs. 2 and 3 indicates that the γ state is filled slowly since CO adsorbed at 120 K is not converted during the desorption ramp of Fig. 2 (10 K/s). Another difference in Figs. 2 and 3 occurs on the low temperature side of the spectrum; there is no β desorption in Fig. 3. The adsorption temperature, 285 K, lies within the β CO desorption peak profile. Thus not all of the β -CO sites would have been populated. We conclude that β sites are not thermally stable when CO is adsorbed at 285 K and speculate that their thermal activation leads to the formation of γ -CO.

For comparison, we examined Rh overlayers on Al_2O_3 . Upon annealing above 450 K, these layers sintered, losing surface area and exposing Al_2O_3 .

This is a common occurrence for supported metals. That Rh on TiO_2 becomes flatter, losing surface area, upon annealing to 600 K, is therefore significant. This result is reminiscent of microscopy results which were explained in terms of enhanced surface wetting of Pt on reduced TiO_2 surfaces [4]. Regardless of the mechanistic details, reduced Ti species tend to stabilize the Rh- TiO_2 interface.

The linear relation between CO adsorption and TiO_x coverage (Fig. 2) supports site blocking as the primary mechanism for CO uptake reduction. This conclusion must be qualified: extensive low coverage TiO_x data was not acquired because precise control of TiO_x coverage was not possible in this regime.

Perhaps the most interesting observations are the two new CO desorption states, β and γ . The development of these desorption states on the encapsulated surface indicates that surface TiO_x is indeed affecting the surface chemistry of Rh.

III.2 NO on Rh/ TiO_2

Typically NO dissociates on Rh at about 275 K [35,36,37]. Low initial NO coverages dissociate completely, desorbing as N_2 and O_2 . For high NO exposures, some molecular NO desorbs. Figure 4 presents the results for desorption of NO (10L, 120 K) from a clean (no encapsulation) 30 Å Rh/ TiO_2 sample (^{15}NO was used throughout). Two NO desorption peaks (130 and 436 K), three N_2 peaks (198, 450 and 650 K), and a small N_2O peak (166 K) were detected. In repeated experiments, the high temperature N_2 peak positions were constant within ± 5 K, the NO peak was always at 436 ± 2 K and the area ratio NO/N_2 was constant to within 20%. These variations may reflect small changes in the morphology of the Rh overlayer depending on uncontrolled

preparation details. Oxygen desorption from these surfaces was not observed because the experiments were limited to less than 800 K (oxygen desorbs from Rh at about 1200 K). The data in Fig. 4 compare quite well with NO desorption from single crystal Rh surfaces. The small N_2O peak in Fig. 4 may be either from NO decomposition on parts of the sample exposing TiO_2 or from a small contaminant.[33]

After characterization of NO desorption from clean Rh surfaces, the Rh layer was encapsulated by heating to 735 K. This temperature was chosen to partially encapsulate the Rh layer with TiO_x while still providing exposed Rh atoms for NO adsorption. The TPD data (Fig. 5) shows some striking differences compared to the clean surface results. Most importantly, the low temperature N_2O desorption peak dominates the spectrum. This N_2O must be from reaction of adsorbed NO, since N_2O is, at most, only a minor contaminant in the NO supply. NO and N_2 desorb at temperatures very near those observed from the clean Rh surface, but the total NO adsorption is reduced by about 50%. This is expected since TiO_x blocks surface Rh atoms. If the sample is annealed at a slightly higher temperature (760 K) for 5 minutes, NO adsorption is reduced by 80% with N_2O still the dominant peak. Since encapsulation reduces the total uptake, NO does not adsorb significantly on TiO_x . However, TiO_x does promote the dissociation of NO at low temperature.

Less than saturation NO exposures were also examined on this partially encapsulated Rh surface. NO dissociates completely upon TPD of a 0.5 L NO dose adsorbed at 110 K. While complete NO dissociation is observed on Rh single crystals, very little N_2O is observed, whereas it is the primary desorption product from encapsulated surfaces. There is no shift in the N_2O desorption temperature (150 K) as a function of NO exposure, suggesting that

N_2O desorption is first order. Possible explanations are that N_2O is formed below the temperature where desorption occurs, or that N_2O desorption originates from reaction of a N-NO complex similar to that proposed for N_2 formation on polycrystalline Rh.[36] Regardless of the interpretation, the important point is that TiO_x enhances low temperature NO dissociation leading to N_2O formation.

Consecutive NO desorptions were performed from the encapsulated Rh surface. Even on the fifth desorption cycle, N_2O was still the major product. The results are complicated by the continual migration of TiO_x to the Rh surface during the course of TPD. AES data taken after each of the five desorption experiments showed an increase in the Ti/Rh ratio; however, the O/Ti ratios remained nearly constant. In separate, X-ray photoelectron analysis, there is evidence for the slow oxidation of Ti to Ti^{4+} . SSIMS isotope experiments using labeled oxygen confirm that oxygen from NO does become incorporated into the TiO_x on the Rh surface. On balance, these results point to a model where at least two processes occur concurrently: (1) TiO_x is slowly oxidized to TiO_2 by exposure to NO, and (2) $\text{N}_{2\text{O}}$ is formed from NO, probably at special sites where Rh, Ti and O all interact (for example, perimeter sites).

These experiments probe the interactions in the NO-Rh- TiO_x system and show a strong effect of TiO_x on Rh surface chemistry. The extent to which the effect (N_2O formation) is due to a direct TiO_x -NO interaction is not clear, but these species certainly alter the reaction paths for NO on Rh. Thus, a full description of SMSI involves more than just blocking Rh sites.

III.3 H_2 on Pt/ TiO_2

The results from NO and CO chemisorption examined the chemistry of a

Rh-TiO_x surface. One question that invariably arises is: Is the interaction long range (typically defined as beyond nearest neighbor distances) or short range? Answering questions such as this, even on ideal systems such as K/Ni(100), [34] is extremely difficult. Since our control, calibration and ability to maintain specific TiO_x coverages was somewhat limited, we designed an experiment to separate site blocking effects from through-metal interactions. To do this, it was necessary to establish the metal-TiO_x interaction, or bonding, without removing metal surface adsorption sites. In this experiment Pt was used instead of Rh because it is slightly more stable than Rh with respect to encapsulation. [26] Small amounts (about 1 ML) of Pt were vapor deposited on TiO₂ substrates (both sputter reduced and fully oxidized). Then H₂ was adsorbed at 120 K, followed by H₂ TPD. During H₂ desorption the maximum temperature reached was 400 K (below the temperature of encapsulation and treated here as annealing the sample). After desorption from the as-deposited Pt layer, a second 10 L H₂ desorption experiment was performed to confirm the first result. The desorption experiments were complemented with AES data to monitor the Pt/Ti ratio (within the AES sampling depth) during the course of the desorption experiments.

Figure 6 shows the results for the adsorption of H₂ onto a 0.7 ML Pt on a fully oxidized TiO₂ sample. Spectrum (a) is the first 10 L desorption and (b) is the second. AES data were acquired after deposition of the Pt layer and after each of the two desorptions. The desorption peak maximum (273 K in (a)) agrees well with data for 30 Å Pt/TiO₂ samples studied in this work, indicating no perturbation of the Pt layer by the underlying TiO₂ substrate. We assume no H₂-Pt-TiO₂ reaction during desorption, which seems reasonable at these low temperatures. The second H₂ desorption has a different shape

and 25% less overall area than the first. The second TPD also shows two peaks, one at about 225 K and another at 295 K. AES after the second thermal desorption shows that the Pt/Ti ratio has changed from 1.6 (before the first TPD) to 1.1. The loss of surface Pt signal is discussed below.

The upper panel of Fig. 6 shows the data for 0.9 ML Pt on prereduced TiO_2 ; experimental procedures were identical to those in the fully oxidized case. The entire data set was obtained in less than 10 minutes (from the time that Pt was dosed to completion of the third AES spectrum). Keeping the time as small as possible assured that CO contamination was not affecting the results. Spectrum 6c (the first desorption) is characterized by a desorption maximum (250 K) about 25 K lower than that observed for H_2 desorption from thick (30 Å) clean Pt overlayers. After annealing to 400 K (the first desorption) and redosing H_2 , the peak area decreased by 60% (Fig. 6d). After annealing, the peak position dropped but its determination in spectrum 6d was difficult because of the width of the very small desorption peak. A Pt/Ti AES ratio of 1.85 was observed before and after the first desorption experiment, indicating no major change in surface distribution of Pt and Ti.

Figure 6 shows that Pt supported on reduced TiO_2 has reduced chemisorption capacity relative to Pt supported in fully oxidized TiO_2 . Structural rearrangement of the reduced Pt/ TiO_2 sample was not detected by AES; therefore, encapsulation was not responsible for the 60% chemisorption suppression on the reduced sample. The change in Pt/Ti ratio observed upon annealing the oxidized Pt/ TiO_2 sample was easily measurable and qualitatively reproducible, indicating that a structural rearrangement (probably islanding) accounts for the 25% reduction in H_2 adsorption capacity. Encapsulation of the oxidized sample is ruled out because: (1)

encapsulation was not observed below 600 K for thicker Pt on TiO_2 , (2) SSIMS and AES measurements showed encapsulation occurred at lower temperatures on the reduced samples, (3) no Ti AES lineshape change was observed in the oxidized samples (a lineshape change was always observed upon encapsulation), and (4) there is good evidence for islanding of Pt on single crystal $\text{TiO}_2(110)$ [39]. While it is not possible to rule out interdiffusion of Pt and oxidized TiO_2 as responsible for the loss of surface Pt atoms, no evidence for it was found in depth profile analysis of other samples. Turning to the reduced sample, since no significant change in the AES Pt/Ti ratio was observed, while there was a 60% reduction of H_2 chemisorption, we look to Pt-Ti-O chemistry. One explanation is that during annealing to 400 K (the first desorption), bonds were formed between Ti and Pt atoms that altered the chemistry of those Pt atoms. Formation of Pt-Ti bonds is proposed for three reasons: (1) 400 K is well below the temperature at which Pt oxides can be formed, (2) the surface is oxygen deficient, leaving many "unsaturated" Ti atoms, and (3) Pt-Ti bonds are 5 Kcal/mole stronger than Pt-Pt bonds [38]. Formation of Pt-Ti intermetallics is not a new concept in the field of SMSI [3].

These experiments were repeated five times. In all cases the results were qualitatively the same. The second TDS for the reduced sample showed at least a 60% decrease in H_2 desorption peak area, while oxidized samples were reduced about 30%. For the reduced sample, annealing to 400 K prior H_2 adsorption lowers the desorption maxima to 215 K. Annealing the oxidized samples splits the single H_2 desorption peak into one at lower and one at higher temperatures.

The above data is consistent with the following phenomenology: (1) Pt deposited on reduced TiO_2 at 110 K is modified slightly, yielding H_2

desorption temperatures 20 K below normal, (2) when annealed to 400 K, Pt-Ti-O bonds are formed (activated process) at the Pt-TiO₂ interface, and (3) after formation of the Pt-Ti-O species the surface Pt atoms have significantly less affinity for H₂ and CO. In the absence of reduced Ti species, the Pt-support interaction is weaker, so when the system is annealed to 400 K, Pt-Pt interactions lead to some islanding. Islanding lowers the chemisorption capacity due to loss of Pt surface area. At higher temperatures (650 K), encapsulation occurs on both oxidized and reduced surfaces. However, as reported elsewhere, encapsulation is more difficult on high quality (single crystal), fully oxidized TiO₂ [39].

IV. Summary and Extrapolation

The effects of TiO_x encapsulation are summarized as: (1) TiO_x blocks metal atom (Pt or Rh) adsorption sites for H₂, CO and NO adsorption, (2) TiO_x induces a low temperature CO desorption state when CO is adsorbed at 120 K, (3) in the presence of TiO_x, adsorption of CO at 285 K leads to the formation of a new form of CO that desorbs at 685 K, (4) TiO_x increases the low temperature NO dissociation on Rh and enhances low temperature N₂O desorption at 165 K, and (5) TiO_x lying under submonolayer amounts of Pt reduces H₂ adsorption without blocking Pt atom adsorption sites.

These results provide direct evidence of strong chemical interactions between adsorbates and surface TiO_x and confirm that TiO_x is not simply a site blocking agent in SMSI catalysts. The CO and NO chemisorption results suggest that TiO_x is active for dissociation reactions. These TiO_x-associated dissociation sites may be associated with the enhanced methanation activity of SMSI catalysts. To confirm this speculation,

quantification of the number of TiO_x sites and correlation with methanation activity is required.

Another important result is the isolation of an effect on Pt due to the presence of underlying TiO_x . The results indicate that TiO_x can influence a Pt atom (or group of atoms) located over it.

The results from these model catalyst studies can be extrapolated to suggest the following working model for the characteristics of powder SMSI catalysts: (1) decreases in H_2 and CO uptake observed upon high temperature reduction are due mainly to site blocking from encapsulating TiO_x , (2) TiO_x also modifies the surface to give new CO adsorption sites, (3) on the metal particles there are two types of sites, "clean metal" sites and highly reactive TiO_x -metal related sites, and (4) the TiO_x sites enhance CO dissociation which, in turn, enhances methanation activity.

References

1. S. J. Tauster, S. C. Fung and R. L. Garten, J. Am. Chem. Soc. 100(1978)1706.
2. S. J. Tauster, S. C. Fung, R. T. K. Baker and J. A. Horsley, Science 211(1981)1121.
3. J. A. Horsley, J. Am. Chem. Soc. 101(1979)2870
4. R. T. K. Baker, E. B. Prestidge and R. L. Garten, J. Catal. 56(1979)390.
5. R. T. K. Baker, E. B. Prestidge and L. L. Murrell, J. Catal. 79(1983)348.
6. M. A. Vannice and C. C. Twu, J. Catal. 82(1983)213.
7. D. E. Resasco and G. L. Haller, J. Catal. 82(1983)279.
8. R. Burch and A. R. Flambard, J. Catal. 78(1982)389.

9. H. R. Sadeghi and V. E. Henrich, J. Catal. 87(1984)279.
10. D. N. Belton, Y.-M. Sun and J. M. White, J. Phys. Chem. 88(1984)5172.
11. Metal-Support and Metal Additive Effects in Catalysis, B. Imelik et al., eds., Elsevier (Amsterdam 1982).
12. Y.-W. Chung, G. Siong and C. C. Kao, J. Catal. 85(1984)237.
13. X.-Z Jiang, T. F. Haden and J. A. Dumesic, J. Catal. 83(1983)168.
14. G. C. Bond, "Catalysis by Metals." Academic Press, London/New York, 1962.
15. R. L. Moss and L. Whalley, Advances in Catalysis and Related Subjects, 22(1972)115.
16. K. Hauffe in "Semiconductor Surface Physics" (R. H. Kingston, Ed.) Univ. of Pennsylvania Press, 1957, p. 259.
17. Th. Wolkenstein, Adv. in Catalysis and Related Subjects, 12(1960)189.
18. F. Solymosi, Catal. Rev. 1(1967)233.
19. G. C. Bond and R. Burch, Catalysis 6(1983)27.
20. Y.-W. Chung and S. Takatani, J. Catal. 90(1984)75.
21. R. T. K. Baker, J. J. Chuldzinski and J. A. Dumesic, J. Catal. 93(1985)312.
22. D. N. Belton, Y.-M. Sun and J. M. White, J. Am. Chem. Soc. 106(1984)3059.
23. D. J. Dwyer, S. D. Cameron and J. L. Gland, J. Vac. Sci. Technol. A3(1985)1569.
24. M. A. Vannice, C. C. Twu and S. H. Moon, J. Catal. 79(1983)70.
25. S.-M. Fang, J. M. White and J. G. Ekerdt, J. Catal. (in press).
26. D. N. Belton, Ph.D. Dissertation, University of Texas at Austin, 1985.
27. Y. Zhu and L. D. Schmidt, Surface Sci. 129(1983)107.
28. P. A. Thiel, E. D. Williams, J. T. Yates, Jr. and W. H. Weinberg,

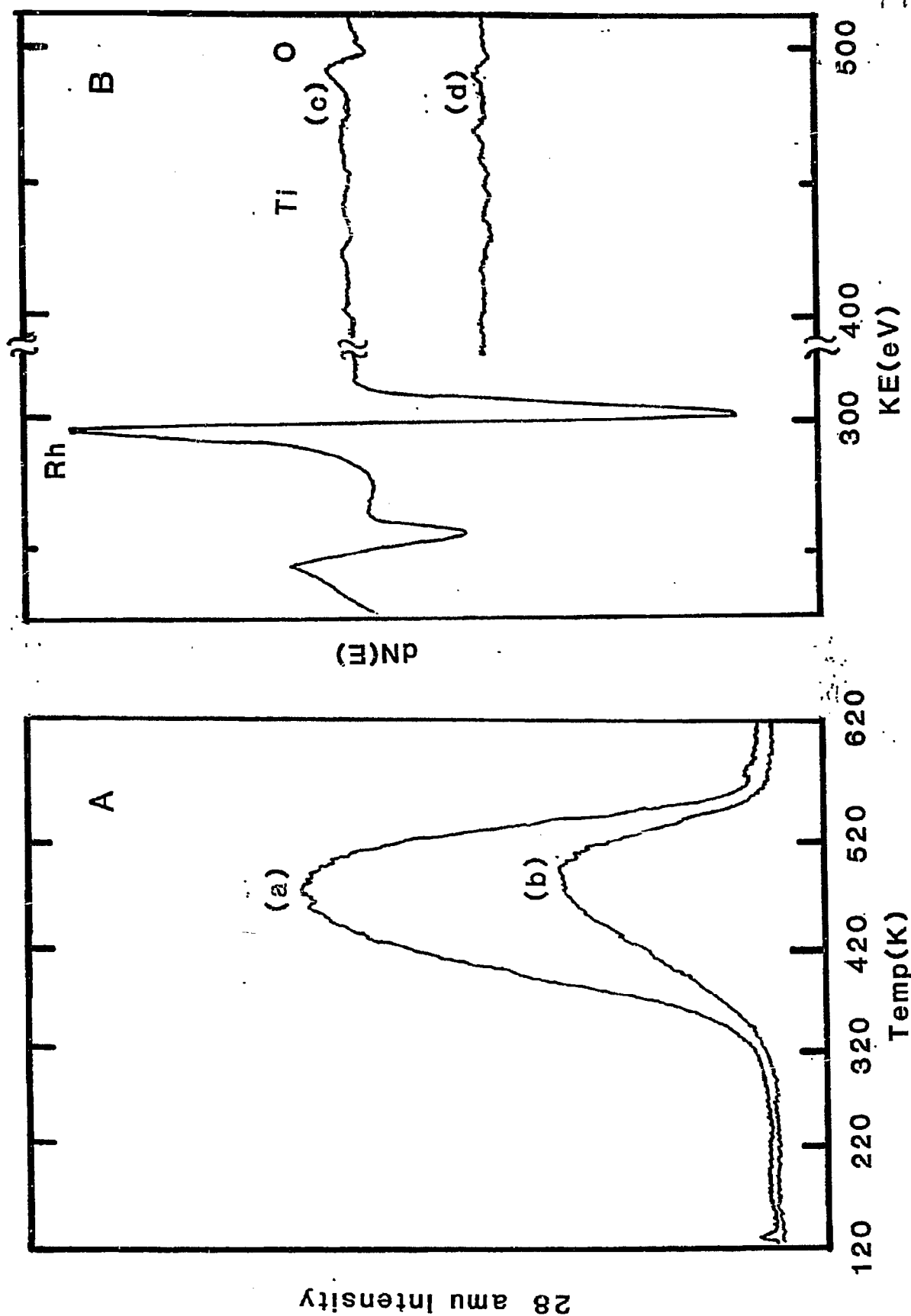
Surface Sci. 84(1979)54.

29. R. J. Baird, R. C. Ku and P. Wynblatt, Surface Sci. 97(1980)346.
30. Y. Kim, H. C. Peebles and J. M. White, Surface Sci. 114(1982)313.
31. T. W. Root, L. D. Schmidt and G. B. Fisher, Surface Sci. 150(1985)173.
32. W. M. Daniel and J. M. White, Surface Sci. (in press).
33. T. W. Root, G. B. Fisher and L. D. Schmidt (submitted).
34. H. S. Luftman, Y.-M. Sun and J. M. White, Appl. Surf. Sci. 19(1984)59.
35. T. W. Root, L. D. Schmidt and G. B. Fisher, Surface Sci. 134(1983) 30.
36. C. T. Campbell and J. M. White, Appl. Surf. Sci. 1(1978)347.
37. P. Ho and J. M. White, Surface Sci. 137(1984)117.
38. M. S. Spencer, Surface Sci. 145(1984)145.
39. Y.-M. Sun, D. N. Belton and J. M. White, J. Phys. Chem. (in press).

FIGURE CAPTIONS

- Fig. 1. TDS (Panel A) of 10 L CO adsorbed at 120K onto a 120 Å Rh/TiO₂ sample. Spectrum (a) is the first desorption from the sample and spectrum (b) is the second. Panel B gives AES data before the first desorption (c) and after the second desorption (d).
- Fig. 2. TDS of 10 L CO from a 30 Å Rh/TiO₂ sample. In the TDS data of the left-hand panel, the sample was annealed to: (a) 600 K, (b) 650 K, (c) 700 K and (d) 760 K. The right-hand panel plots CO desorption peak areas vs. Ti/Rh AES ratios. The measured peak areas are normalized to the desorption area of spectrum (a) in the left-hand panel. The triangles denote the β state.
- Fig. 3. TDS of 10 L CO adsorbed at 270 K onto a 30 Å Rh/TiO₂ sample. Spectrum (a) is CO desorption from the as-deposited Rh layer and (b) is desorption from the Rh/TiO₂ sample after annealing to 780 K prior to CO adsorption at 270 K.
- Fig. 4. TDS of 10 L ¹⁵N₂ adsorbed at 110 K onto a 30 Å Rh/TiO₂ sample. The sample was annealed to 525 K (no encapsulation) prior to N₂ adsorption.
- Fig. 5. TDS of 10 L ¹⁵N₂ adsorbed at 110 K onto a 30 Å Rh/TiO₂ sample which was annealed to 735 K (encapsulation) prior to N₂ adsorption.
- Fig. 6. Two consecutive 10 L H₂ TDS from ~1 ML Pt/TiO₂ samples. Desorption data are for Pt supported on reduced TiO₂(r) (top panel) and oxidized TiO₂(o) (lower panel). Spectrum (a) is before (b) and spectrum (c) before (d).

Fig. 1



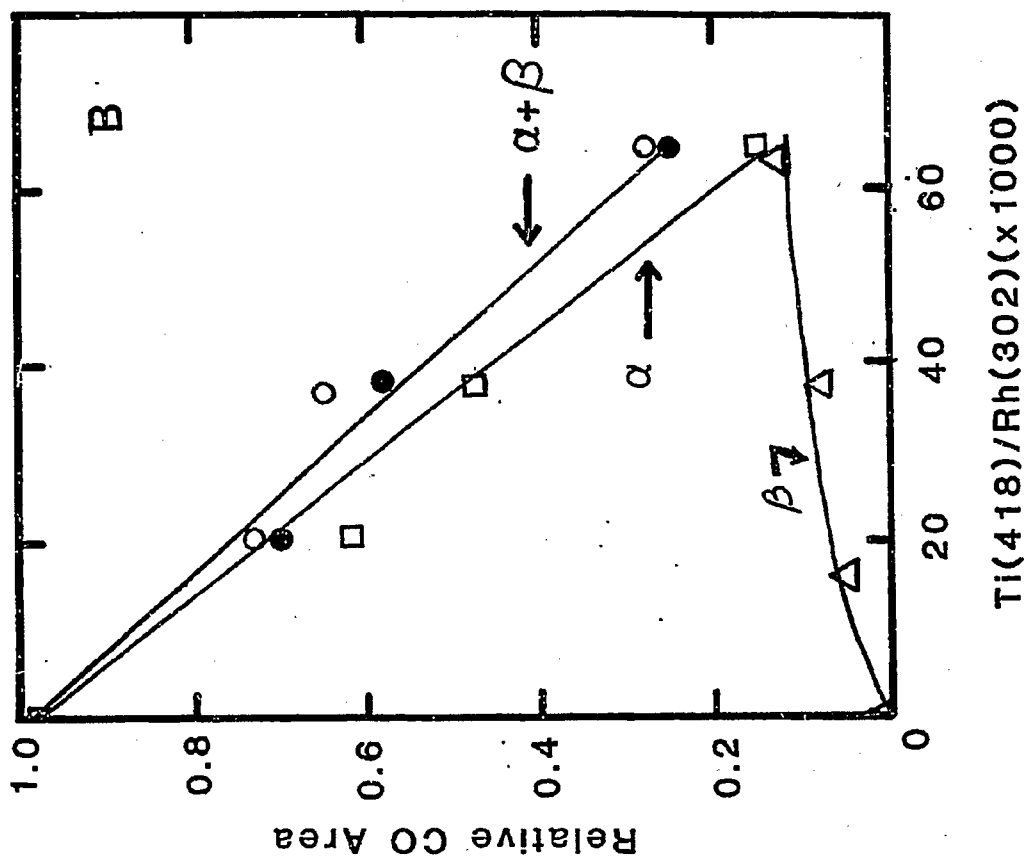
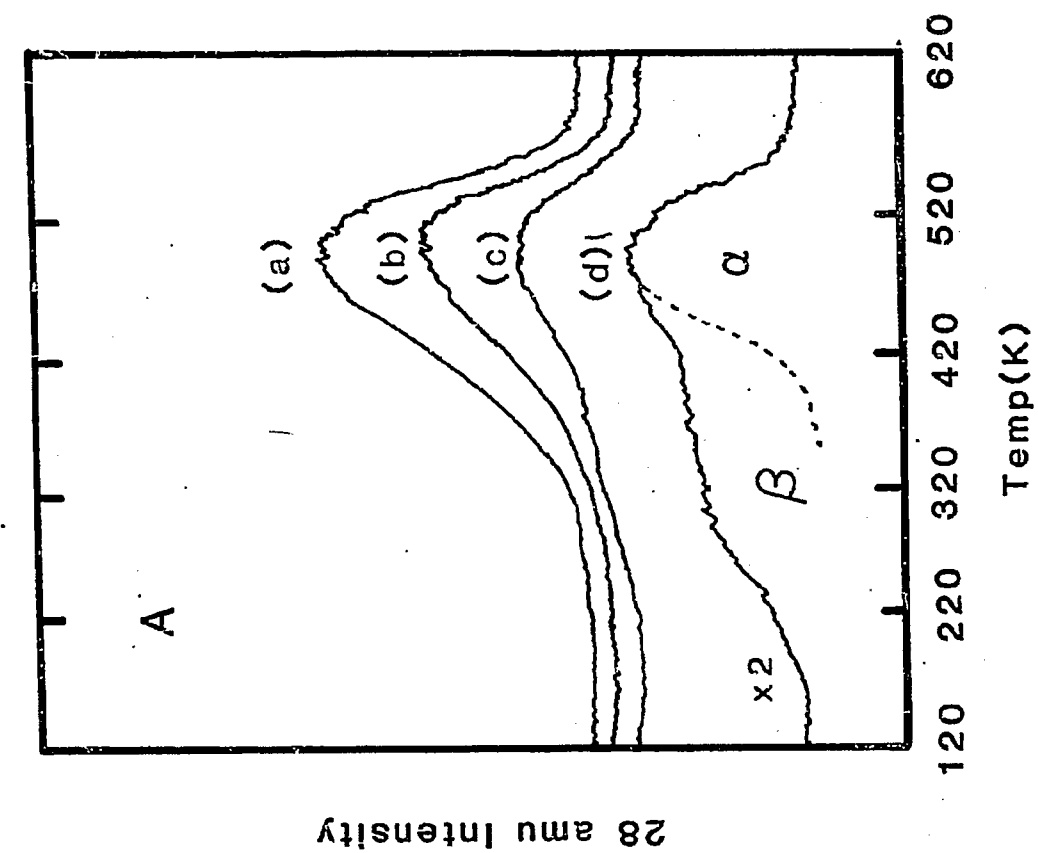


FIG. 2

4

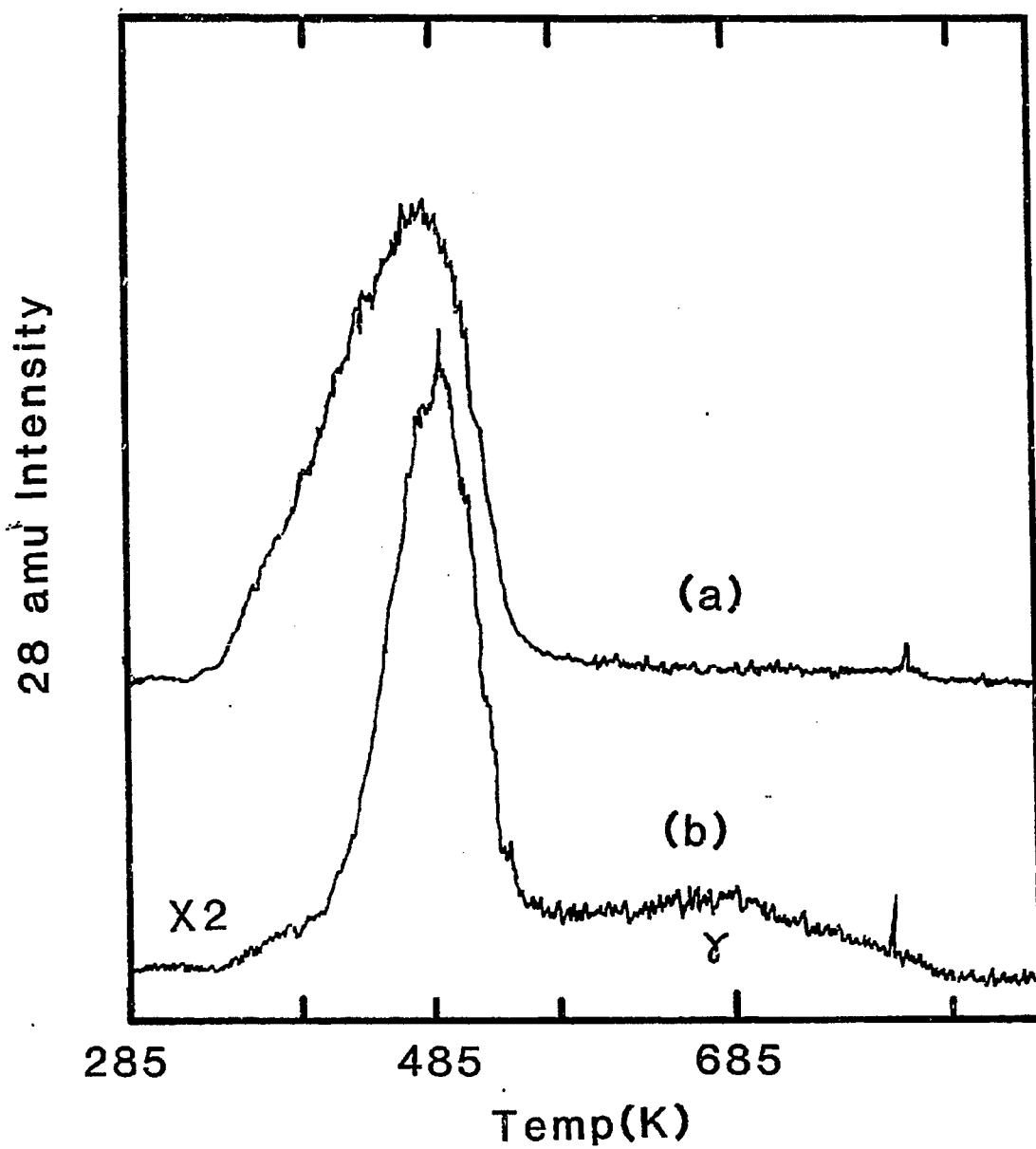


Fig.3

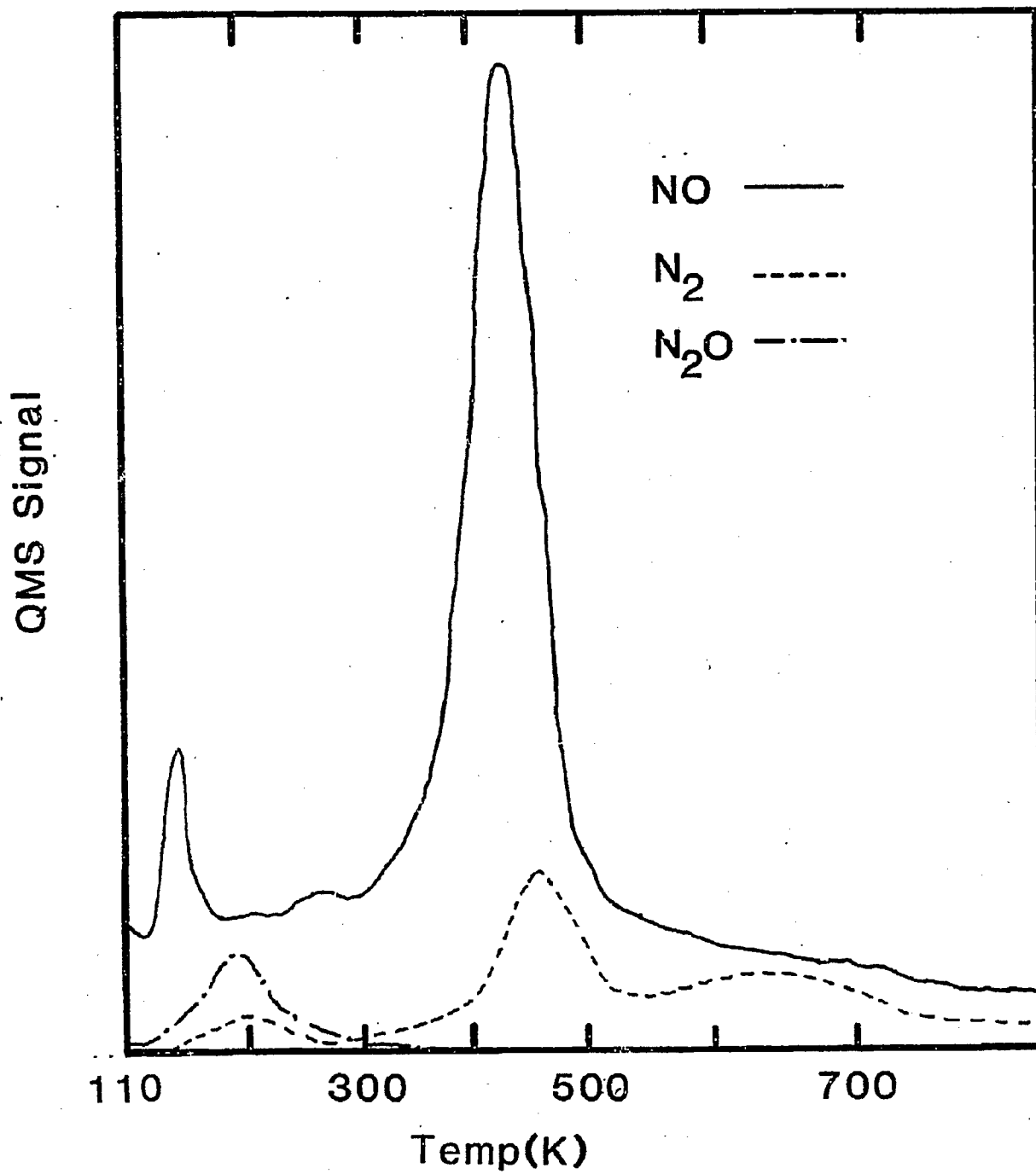
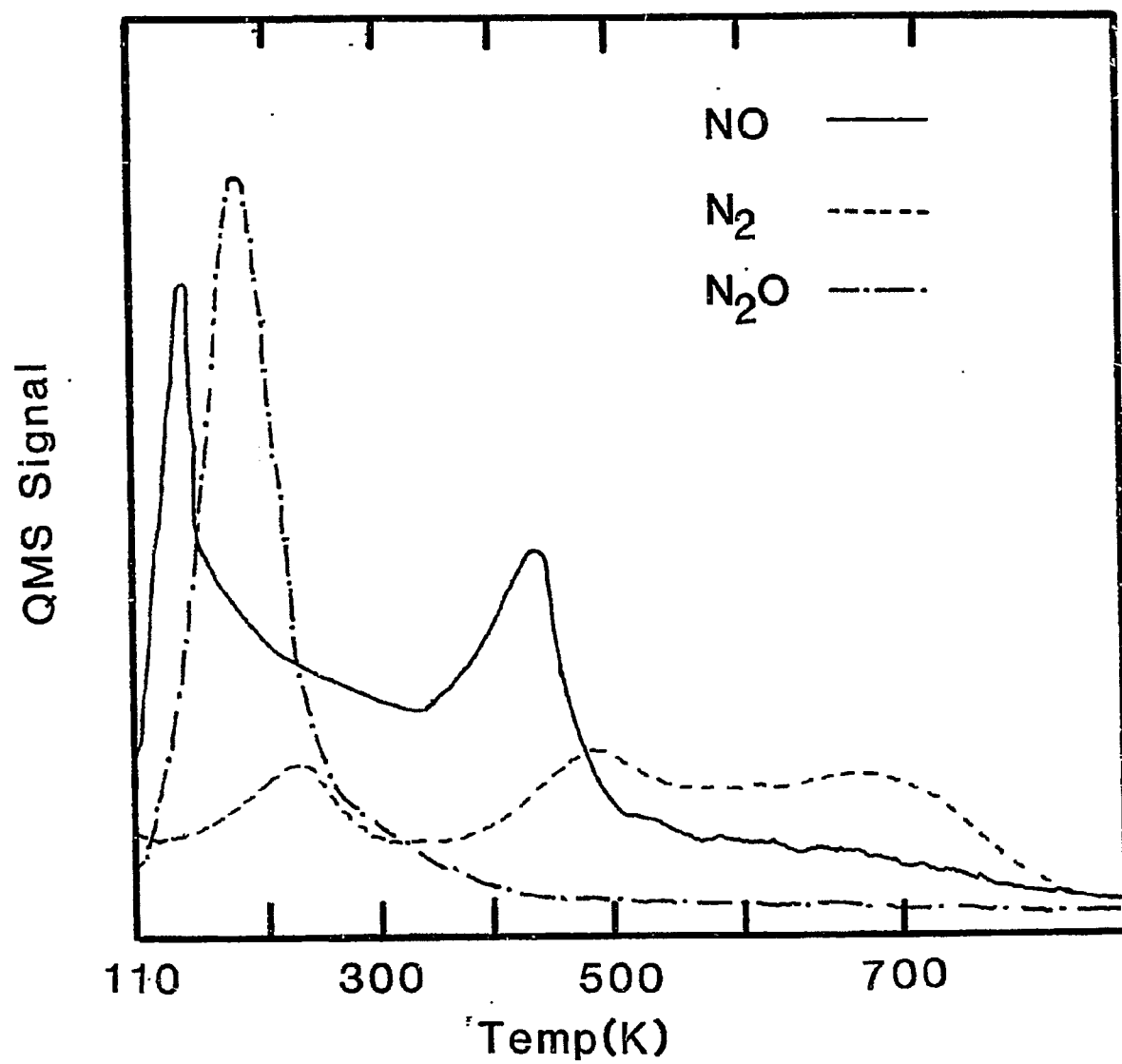


Fig 4

FIG 5



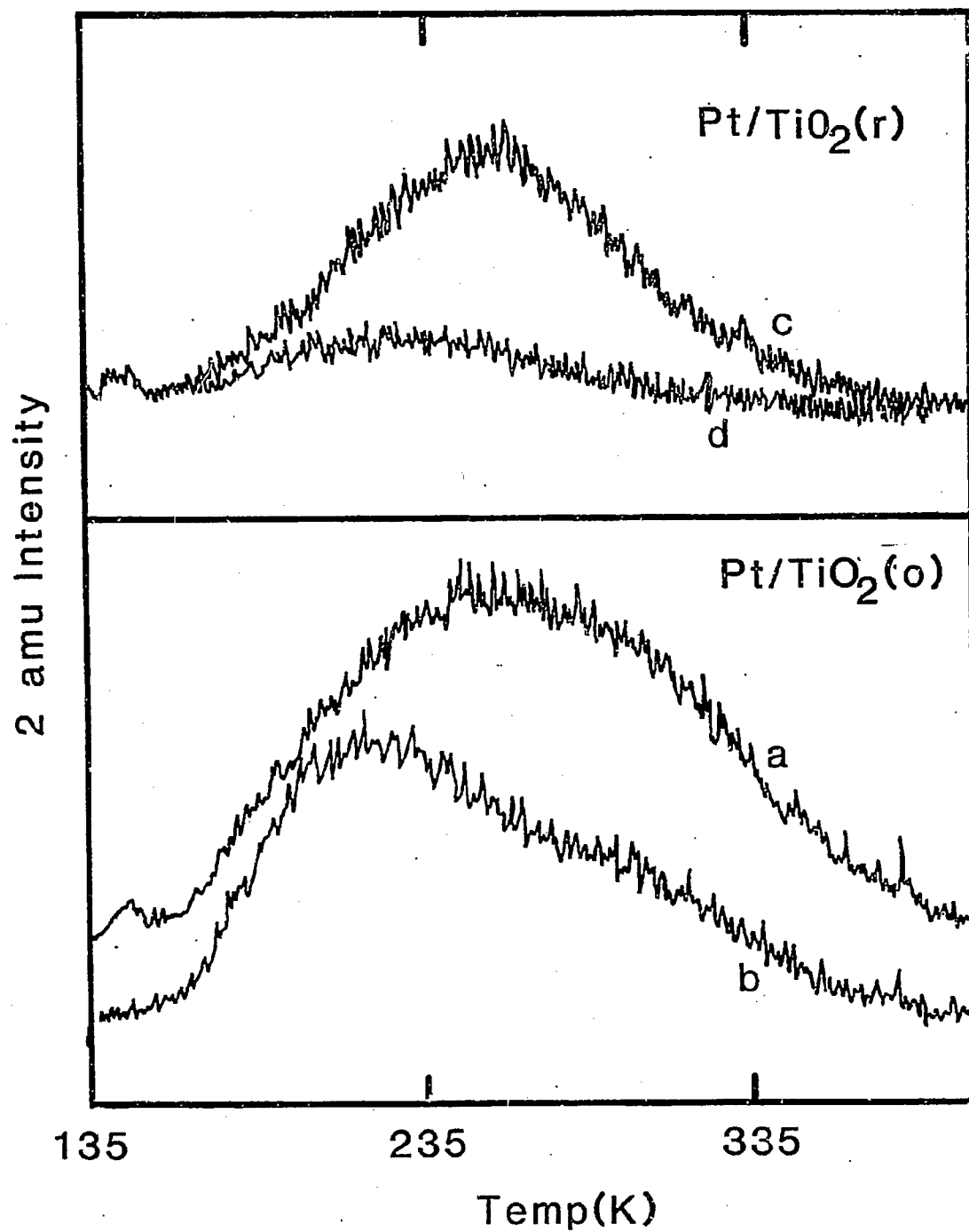


Fig. 6